applied sciences

MDPI

Article

The Effects of Fly Ash, Blast Furnace Slag, and Limestone Powder on the Physical and Mechanical Properties of Geopolymer Mortar

Salih Aslan and İbrahim Hakkı Erkan *

Department of Civil Engineering, Faculty of Engineering and Natural Sciences, Konya Technical University, Konya 42000, Turkey; salih.aslan1028@gmail.com
* Correspondence: iherkan@ktun.edu.tr

Abstract: This study investigates the alterations in the ratios of components such as class C fly ash (FA), blast furnace slag (BFS), and waste stone powder (WSP) types of limestone powder (LP) used in the production of geopolymer concrete. These components are meticulously examined concerning the physical and mechanical attributes of geopolymer concrete. Using the mixture-design method, 10 different mixing ratios were determined using FA, BFS, and LP, and experimental research on the mechanical attributes and workability of geopolymer mortar is presented. A series of experimental tests, including tests for compressive strength, impact strength, setting time, flow table, flexural strength, and water absorption, were carried out on the geopolymer mortars that were made using FA, BFS, and LP, to investigate and enhance their overall performance. The experimental study aimed to ascertain the extent to which variations in the materials used in the formation of geopolymer mortar affected its mechanical and physical properties. To achieve this objective, certain parameters for geopolymer mortar formulation were fixed, according to the literature (molarity: 10; aggregate/binder ratio: 2.5; plasticizer ratio: 2%; sodium silicate (SS)/sodium hydroxide (SH): 1.5; additional water content: 14.5%; alkali activators/binder: 0.5). Subsequently, mortars were produced according to the 10 different mixing ratios determined by the mixture-design method, and the experiments were completed. The samples of the 10 different mixes were subjected to air curing at an ambient temperature (23 °C ± 2 °C) for 28 days. Following the curing period, the tests revealed that mix No. 9 exhibited the best compressive, flexural, and impact strengths, while mix No. 10 demonstrated superior workability of geopolymer mortar. It was shown that impact, compressive, and flexural strength values decreased as the ratios of FA and LP increased. In contrast, the increases in the ratios of FA and LP positively influenced the workability of geopolymer mortar.

Keywords: blast furnace slag; compressive strength; fly ash; geopolymer; impact strength; limestone powder

Citation: Aslan, S.; Erkan, İ.H. The Effects of Fly Ash, Blast Furnace Slag, and Limestone Powder on the Physical and Mechanical Properties of Geopolymer Mortar. *Appl. Sci.* **2024**, *14*, 553. https://doi.org/10.3390/app14020553

Academic Editor: Asterios Bakolas

Received: 7 December 2023
Revised: 4 January 2024
Accepted: 5 January 2024
Published: 8 January 2024

1. Introduction

Geopolymer concrete, developed by Davidovits, offers a viable substitute for traditional concrete [1]. Geopolymer concrete (GPC) is produced from waste materials containing aluminosilicates, activated by alkali activators. Researchers have been paying attention to geopolymer materials recently because of their superior durability, high mechanical and physical qualities, and low carbon dioxide (CO_2) emissions. Excessive use of energy and high release of CO_2 happen when making cement. Accordingly, research efforts have shifted toward alternative binding materials to mitigate environmental impact. Studies indicate that energy costs in cement production account for approximately 20% to 40% of overall costs [2–4]. Research studies have demonstrated that producing one ton of cement emits roughly one ton of CO_2. Annually, global CO_2 emissions from cement plants alone contribute an estimated 5% to 8% to overall CO_2 emissions [5].

In recent years, there has been a growing emphasis on recycling industrial waste materials such as fly ash, blast furnace slag, and waste stone powder (WSP). These materials can be activated with various alkalis, resulting in the production of binding materials used in geopolymer concrete [6–12].

According to American Material Test Standard (ASTM) C618-19, fly ashes obtained from bituminous coal, with a content of SiO_2 + Al_2O_3 + Fe_2O_3 exceeding 50%, are classified as class C. Furthermore, in the class C fly ash classification, it has been indicated that the calcium oxide (CaO) content is above 10%. The fly ash chosen in this study was class C fly ash [13].

Polymerization is a heterogeneous chemical reaction. The exposure of aluminosilicate hydrates to heat causes the dissociation of OH ions, forming water, and initiates the formation of Si-O-Al bonds [14]. This reaction, occurring between solid aluminosilicate oxides and alkali metal silicate solutions under highly alkaline conditions and moderate temperatures, results in amorphous semi-crystalline polymeric structures containing Si-O-Al and Si-O-Si bonds [15].

Various geopolymers have been defined in the literature based on the Si/Al ratio. Some of these include water glass-based geopolymer, polysiloxonate (Si:Al = 1:0), kaolin hydroxysodalite-based geopolymer, polysialate (Si:Al = 1:1), metakaolinite-based geopolymer, poly (sialate-siloxo) (Si:Al = 2:1), calcium-based geopolymer, (Ca, K, Na)-sialate, (Si:Al = 1, 2, 3), rock-based geopolymer, poly (sialate-multisiloxo) ($1 < Si:Al \leq 5$), and fly ash-based geopolymers [16].

Potassium hydroxide (KOH), potassium silicate (K_2SiO_3), sodium hydroxide (NaOH), and sodium silicate (Na_2SiO_3) are utilized as alkali activators in the activation processes [17–20]. In geopolymers produced through alkali activation, the C-S-H gel observed in traditional Portland cement is replaced by N-A-S-H or C-A-S-H gel [21,22]. The influence of this gel is crucial in the strength mechanism of geopolymers. Additionally, the Si/Al ratios in the structure of binders used in the mixture also impact the bonding structure [23,24]. Generally, heat curing is required for geopolymers to gain strength [25–27]. While 60–80 °C is sufficient for BFS and metakaolin-based geopolymers [28,29], FA-based geopolymers require a temperature range of 80–110 °C [17,30]. Factors such as curing temperature, curing duration, binder quality depending on coal combustion, binder content, aggregate type, water amount, activator ratio, activator type, and curing conditions are important in the strength mechanism [17,31–33]. Geopolymer concretes exhibit early and high strength, high-temperature resistance, freeze–thaw resistance, resistance to wetting-drying cycles, and abrasion resistance compared to traditional concretes. They also demonstrate lower drying shrinkage [34,35]. However, some studies indicated lower resistance to acids and sulfates than traditional concretes [36]. Conversely, resistance to acids and heavy metals was reported in certain studies [37,38]. According to the literature, a high CaO content in binders is necessary to perform curing at room conditions. Therefore, FA, BFS, and LP were used in this study. Furthermore, LP was employed to enhance the workability and early setting time of geopolymers [39].

In a study of the physical properties of geopolymer mortar using C-class fly ash, Kotwal et al. reported in 2015 that the density increases and the flow and compressive strength decrease when the percentage of FA increases [40]. Kaya et al., in their 2020 study, found that using FA resulted in an improved compressive strength [31]. In their 2019 study, Sasui et al. further revealed that an increase in FA content led to a decrease in setting time [41]. Moreover, in 2010, Kumar et al. investigated the effect of BFS on fly ash-based geopolymer characteristics and proved that an increase in BFS percentage led to an increase in compressive strength and a decrease in setting time [42]. Ozodabas et al. reported in 2013 that compressive and flexural strength were decreased when the BFS content increased [33]. In 2016, Kürüklü deduced that by increasing BFS, water absorption decreased [43]. The 2021 study of Taher et al. on the effect of LP in geopolymer established that an increase in the amount of LP was accompanied by a decrease in dry unit weight, compressive strength, and flexure strength [44]. In 2017, Bayiha et al. proved that the use of LP in high proportions

leads to a decrease in compressive strength, flexure strength, and water absorption and an increase in setting time [45]. In 2021, Kubatova et al. deduced that the setting time increased at the same time the compressive strength and flexure strength decreased when the percentage of LP increased [46].

The meticulous choice of materials holds utmost significance in geopolymer production, exerting a profound impact on the ensuing material characteristics. Through a thorough investigation, the authors identified a conspicuous gap in the existing literature concerning the simultaneous incorporation of FA, BFS, and LP materials in the production of geopolymers. For instance, extant research has explored the synergistic utilization of FA and BFS in combination [10–12], the exclusive use of FA [16,17,23,27], the exclusive utilization of BFS [15–33], and the exclusive use of LP [39,45,46]. There remains a need for exploration into the combined incorporation of all three materials. This study endeavors to explore the impact and degree of effectiveness on geopolymers' properties when these waste materials are used collectively. Simultaneously, the objective is to fabricate a geopolymer characterized by both heightened performance and good workability.

In this study, aimed at promoting wider utilization of geopolymer concrete and increasing sustainability interest in the construction sector, mortars produced using the mixture-design [47] method underwent various physical tests, such as tests for flow table, unit weight, water-absorption rate, and setting time. Additionally, flexural, impact and compressive strength tests were conducted. The effects of the utilized waste materials on geopolymer mortar were examined. Simultaneously, the mixtures were optimized, determining the optimal mixing ratio concerning their physical and mechanical properties.

2. Materials and Experimental Procedure

2.1. Materials

2.1.1. Fly Ash (FA)

Fly ash is a significant byproduct transported through flue gases resulting from the combustion of pulverized coal in thermal power plants, collected in cyclones or electrostatic filters. The molten material formed due to the high-temperature combustion of coal cools down and transforms, through gas flow, into partially or completely spherical ash particles. These ash particles are very fine (0.5–150 microns) and are referred to as fly ash, due to their being carried by flue gases. The major components found in fly ash include silicon dioxide (SiO_2), aluminum oxide (Al_2O_3), iron (III) oxide (Fe_2O_3), and CaO, and their quantities vary depending on the type of fly ash. The fly ash used in this study is class C fly ash, containing high calcium oxide according to American Material Test Standard (ASTM) C618 [13]. The class C fly ash used in this investigation comes from the Soma Thermal Power Plant in Manisa, Turkey, as shown in Figure 1. In terms of grain size, 11.7% of FA passes through a 90 µm sieve, while 26.6% passes through a 45 µm sieve; the density of FA used in this study was 2.40 g/cm^3. Its chemical and physical properties are provided in Table 1.

(**a**) (**b**) (**c**)

Figure 1. The geopolymer mortar's waste aggregate: (**a**) FA, (**b**) BFS, and (**c**) LP.

Table 1. The nominal chemical composition of BFS, FA, and LP.

Oxides (%)	SiO_2	AI_2O_3	Fe_2O_3	CaO	SiO_2/AI_2O_3	MgO	K_2O	SO_3	MnO	TiO_2
FA	28.05	13.93	6.55	45.09	2.01	-	2.12	3.45	-	0.78
BFS	35.00	16.00	1.40	37.50	2.18	5.25	-	-	1.75	-
LP	4.08	1.62	0.58	43.00	2.51	9.34	0.19	-	-	0.11

2.1.2. Blast Furnace Slag (BFS)

Slags are a waste-material group obtained from various metallurgical facilities. Their chemical compositions and properties vary significantly, depending on the main product type produced by the industrial establishments and the production method used. Slags offer many possibilities for use in the cement and concrete sectors. Slags obtained through conventional steel-production techniques appear as masses with a crystalline structure. Such slags are either discarded without use or employed as road materials or concrete aggregates. Conversely, in facilities employing modern technology for steel production, slags with a glassy structure and some hydraulic properties are obtained. It is possible to utilize these in cementitious systems. Among all types of slags, BFS is the most important and widely used. The BFS used in this study was sourced from the Iskenderun plant of Adana Cement Inc. in Turkey (Figure 1). In terms of grain size, only 0.3% of BFS passes through a 90 μm sieve, while 3.9% passes through a 45 μm sieve; the density of BFS is 2.85 g/cm^3. The chemical and physical properties of BFS are presented in Table 1.

2.1.3. Limestone Powder (LP)

In asphalt factories, aggregates of specific gradations are introduced into high-temperature furnaces (at 150 °C) for a designated duration. Subsequently, these aggregates undergo heating, and the dust particles that form on their surfaces are vacuumed, thereby acquiring the quality of waste material, which is then stored. The resulting LP, formed through the natural process of subjecting these aggregates to heat, attains high pozzolanic activity (at 75%) without the need for additional energy input. Consequently, the acquisition of waste material with high pozzolanic activity, achieved without the requirement of extra energy, holds significant importance in terms of both environmental and energy considerations.

The LP utilized in this study was sourced from the asphalt plant of Konya Meram Municipality in Turkey (Figure 1). In terms of grain size, only 0.7% of LP passes through a 90 μm sieve, while 4.5% passes through a 45 μm sieve. Its density is 2.70 g/cm^3. The chemical characteristics pertinent to LP are provided in Table 1.

Figure 1 illustrates the waste-binding materials employed in this investigation.

2.1.4. Alkali Activators

To start the polymerization process, a chemical activator is needed. Geopolymers are often aluminosilicate binding materials that are activated by silicates or alkaline hydroxides in settings with high pH [48].

1. The polymerization procedure in this research used sodium hydroxide (NaOH) and sodium silicate (Na_2SiO_3) solutions as alkali activators. Local sources were contacted in order to obtain these substances. Purified water was used to dissolve sodium hydroxide (NaOH) until the molarity reached 10.
    a. Sodium Hydroxide (NaOH)
2. A part of the heat is usually lost as the NaOH solution is being prepared, and another part is used up when the solution evaporates. Since NaOH is the most accessible and inexpensive alkali hydroxide, it is the preferred option for use as a hydroxide activator in geopolymer synthesis.
    b. Sodium Silicate (Na_2SiO_2)

Among the alkalis utilized in geopolymer formation, the density of Na_2SiO_3 ranges from 1410 to 1435 g/cm^3. The Na_2SiO_3 solution, one of the alkali activators employed in this study, is an alkali with a solid content of 40%, containing Na_2O and SiO_2. The alkali solutions, formed by mixing Na_2SiO_3 and NaOH solutions, were prepared several hours in advance before being used in the study.

2.1.5. Aggregate

In the preparation of geopolymer mortar, quartz sand was used as aggregate. The sand's specific gravity was 2.706, the largest particle diameter was 4.75 mm, and the water-absorption value was 2.07%.

2.2. Procedures

Finding Mixing Ratios

Constrained mixture design allows users to first analyze the effects of the factors on each material feature by carrying out a manageable number of trials [47,49,50].

In this research, three different waste materials—FA, BFS, and LP—were used to produce a geopolymer mortar. A total of ten mixes were designed using the mixture method in the Minitab statistical software program version 19.1. The ranges of binder ratios in Table 2 were chosen after extensive research of the literature on the potential effect of the materials used in this study. According to Altawil in 2022, with a decrease in the percentage of CaO, the compressive strength of the geopolymer decreases [51]; accordingly, in this study, the CaO ratio was maintained at more than 40%. According to Aktürk, LP provides great positive results in the workability and setting time of geopolymers, but a large increase in LP negatively affects the compressive strength [39]; accordingly, a CaO ratio between 20% and 30% was used. In this case, the Si:Al ratio was maintained at more than 2, thus producing a calcium-based geopolymer. These percentages can be used to determine nonlinear associations between factors and characteristics examined in the mixture-design method. Table 2 illustrates the mixing ratios and their control levels, In Figure 2 The blue dots represent the ten selected mixtures representing the mixture binder ratios as defined for this experiment.

Table 2. Binder ratios (%) from mixture-design method.

Mixture No.	Binder		
	FA (%)	BFS (%)	LP (%)
1	55.00	25.00	20.00
2	45.00	35.00	20.00
3	45.00	25.00	30.00
4	50.00	30.00	20.00
5	50.00	25.00	25.00
6	45.00	30.00	25.00
7	48.33	28.33	23.33
8	51.66	26.66	21.66
9	46.66	31.66	21.66
10	46.66	26.66	26.66

2.3. Geopolymer Production

Certain parameters for all prepared mixtures were chosen and maintained, following the literature. These parameters included an aggregate/binder ratio of 2.5, an SS/SH ratio of 1.5, a molarity of 10, a liquid/binder ratio of 0.5, superplasticizer addition at 2% of the total binder, and additional water content at 14.5% of the total binder. The geopolymer mortar specimens produced within the study were consistently cured under similar conditions, maintaining a constant ambient temperature of 23 °C ± 2 °C throughout the entire curing period.

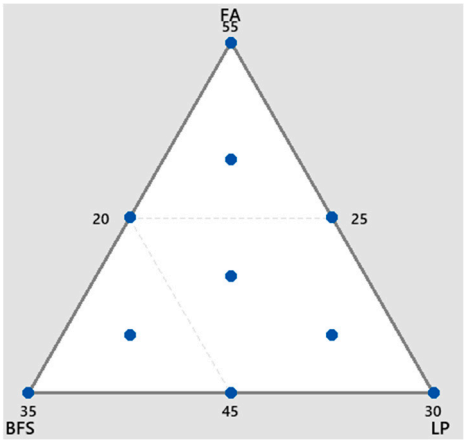

Figure 2. Matrix of simplex design plots.

2.4. Preparation, Casting, and Curing of Test Specimens

From each prepared mixture, three cubes measuring 50 × 50 × 50 mm, six beams measuring 80 × 100 × 400 mm, and three cylindrical specimens with dimensions Ø100/50 mm were prepared. The prepared specimens were cured at room temperature (23 °C ± 2 °C) for 28 days. On the 28th day, the experiments described above were conducted on the specimens (Figure 3).

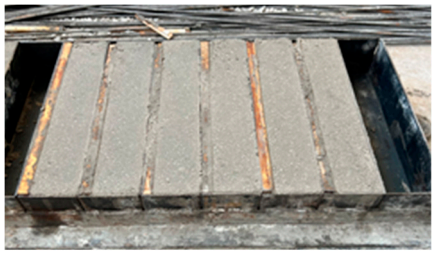

(**a**) Geopolymer beams specimens

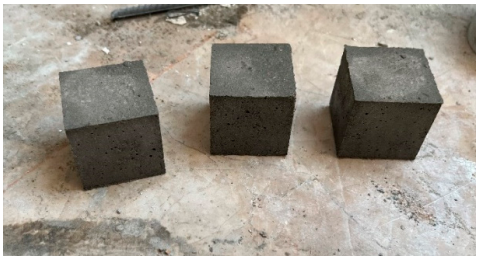

(**b**) Geopolymer cubes specimens

Figure 3. Specimens prepared from geopolymer mortar. Dimensions: 80 × 100 × 400 mm (beams) and 50 × 50 × 50 mm (cubes).

2.5. Property of Tests

The initial and final setting times of geopolymer mortar were measured according to ASTM C 403/C 403 M [52]; a flow table was measured in accordance with ASTM C230 [53]; a compressive strength test was carried out according to ASTM C39-05 [54]; and flexural strengths were obtained according to ASTM C293 [55]. İmpact was measured according to ACI 544 [56] and water absorption was evaluated according to ASTM C642 [57]. Dry unit weights and water absorption of the 28 day specimens were determined using Archimedes's principle. This method involves weight measurements of saturated specimens in air (at 70% humidity) and in water (at 23 ± 2 °C) for 2 days, along with the determination of their dry weights achieved through oven drying at 100 °C for 3 days.

3. Results

3.1. Initial and Final Setting Time of Fresh Mortar

The results of the initial and final times of the geopolymer mortar samples produced in the study are presented in Figure 4 and Table 3. In the experiment conducted to determine the initiation and termination times, it was observed that the initiation times ranged from 12 min to 15.3 min and the termination times ranged from 18 min to 30 min. The mixture denoted as mix No. 2 exhibited the earliest initiation time, whereas mix No. 1 exhibited the longest termination times. With an increase in the quantity of FA, the initiation time of the geopolymer mortar decreased. Consequently, there remained a considerably limited time

for the workability of the geopolymer mortar—an undesirable circumstance. It was found that the inclusion of LP may have yielded favorable results in improving the workability and initiation time of the geopolymer mortar. The experimental results indicated a reduction in setting time and workability as the proportions of FA and BFS increased, as illustrated in Figure 5, which depicts the relationship between the mixing ratio of the materials and the setting time.

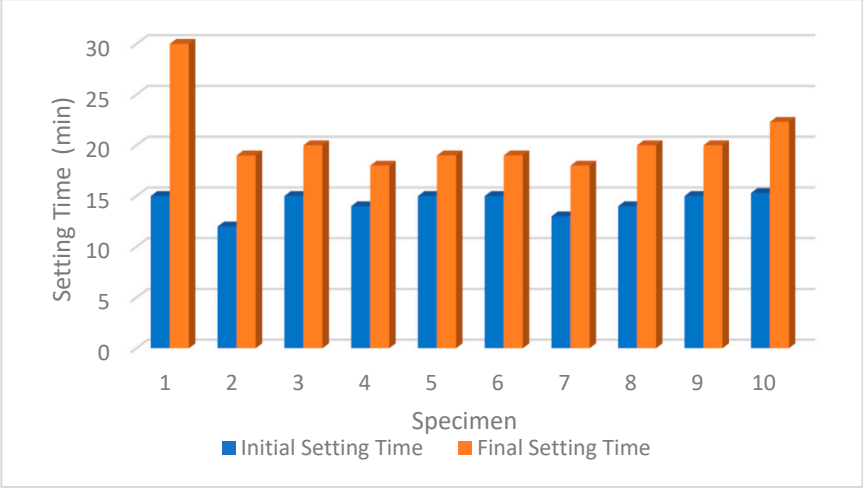

Figure 4. Setting time of the geopolymer mortar.

Table 3. Experimental test results.

Specimen	Initial Setting Time (Min)	Final Setting Time (Min)	Flow Table (mm)	Compressive Strength (MPa)	Flexural Strengths (MPa)	Impact Resistance (kNmm)	Water Absorption (%)	Dry Unit Weight (g/cm^3)
1	15.00	30.00	220.00	7.17	1.98	10.02	10.17	2.06
2	12.00	19.00	185.00	14.61	2.82	30.06	9.02	2.10
3	15.00	20.00	193.00	9.57	2.22	20.04	8.78	2.08
4	14.00	18.00	185.00	12.54	2.02	16.63	9.27	2.07
5	15.00	19.00	180.00	10.10	1.63	16.63	9.49	2.06
6	15.00	19.00	195.00	12.02	1.69	16.63	8.64	2.08
7	13.00	18.00	210.00	14.95	2.55	30.06	8.58	2.09
8	14.00	20.00	200.00	13.69	2.90	33.36	8.87	2.04
9	15.00	20.00	220.00	16.16	2.88	33.36	8.31	2.11
10	15.30	22.30	235.00	14.96	2.52	16.63	8.23	2.08

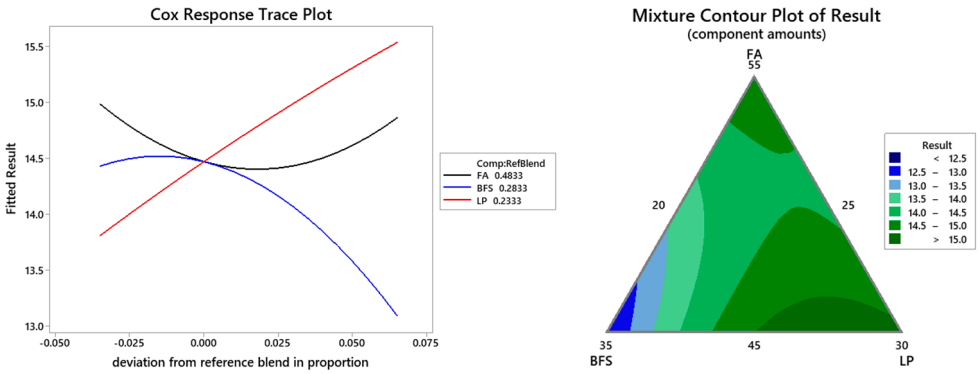

Figure 5. The relationship between the mixing ratio of the material used and the setting time.

In the polymerization process necessary for creating geopolymers, Si-O-Al and Si-O-Si bonds are formed. The binding materials, FA, and BFS, containing a substantial amount of SiO_2, and AL_2O_3, react with the Ca activator solution, resulting in the formation of Si-O-Al

and Si-O-Si bonds, thereby accelerating the polymerization and reducing the setting time by creating Ca-Al-Si gels. Consequently, unlike the hydration of conventional mortar, FA and BFS have been observed to decrease the setting time of geopolymer mortars, a finding consistent with those of earlier studies [41,58–60]. Conversely, LP has been identified to increase the setting time of geopolymer mortars, aligning with similar conclusions drawn in previous research [39,45,46].

3.2. Flow Table

The flow-table test for the geopolymer was conducted following ASTM-C230/C 230M-14. After placing the geopolymer mortar into the mold, the mold was lifted and the handle of the testing apparatus was rotated five times in 15 s. The spread of the mixture was then measured using a meter in two different axes, and the average of the recorded values was noted [53].

The results were determined for all mixtures, and these values are shown in Figure 6. The relationship between mixing ratios and flow-table values is depicted in Figure 7.

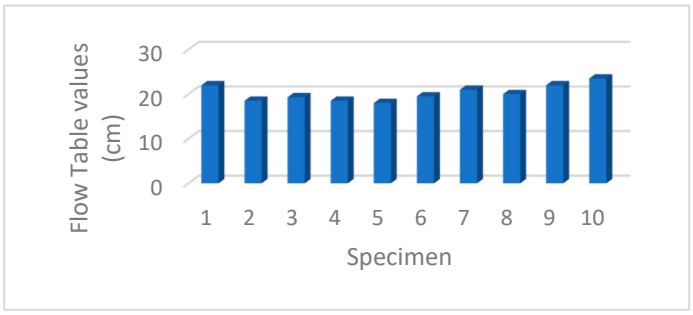

Figure 6. The flow-table values of the geopolymer mortar.

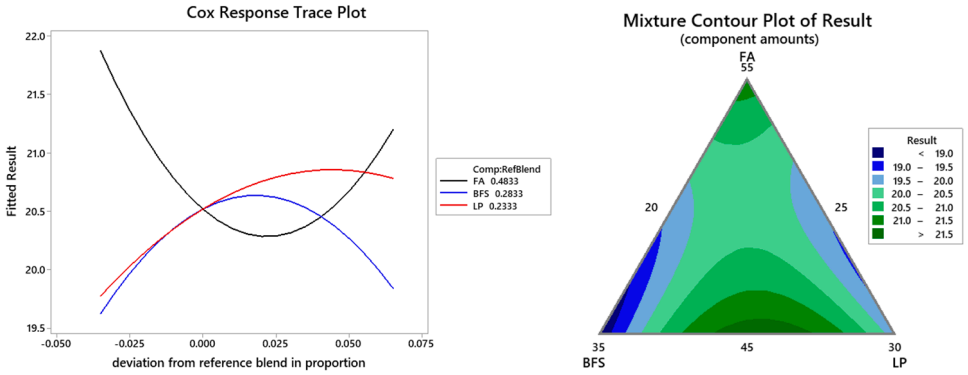

Figure 7. The relationship between the mixing ratio of the material used and the flow-table values.

As shown in Table 3, the results for the mixtures range between 18 and 23.5 cm. Mix No. 10 yielded the best workability, with a value of 23.5 cm.

Polymerization forms Si-O-Al and Si-O-Si bonds. As the FA and BFS quantity in the binder increases, Ca-Al-Si gels form, due to the concurrent increase in SiO_2, AL_2O_3, and CaO content. Consequently, more activator solution is required for the polymerization process, leading to a decrease in flow values. This has been supported in previous studies—i.e., an increase in FA and BFS ratios is associated with a decrease in workability [61–64]. Conversely, an increase in the LP ratio is correlated with an increase in the spread workability value. This result has also been proven in previous studies [65,66].

3.3. Compressive Strength

For the compressive strength test, cubes with dimensions of 50 × 50 × 50 mm were prepared and the experiments were conducted following ASTM C39-05 standards [54]. The 50 × 50 × 50 mm cube samples were subjected to the compressive strength test after a curing period of 28 days, and the obtained results are shown in Table 3.

Upon examining Table 3, it is observed that the compressive strength values ranged from 7.17 to 16.16 MPa. The mixture providing the highest compressive strength value was mix No. 9, with a value of 16.16 MPa. The mixture with the lowest compressive strength was mixed No. 1, with a value of 7.17 MPa. The experiments revealed a decrease in compressive strength with an increase in the ratios of FA and LP. This is believed to be attributable to the presence of undesirable residual materials in the obtained fly ash. Consequently, it was observed that a complete reaction between FA and the activator solution did not occur.

The low SiO_2 and Al_2O_3 content in LP resulted in the formation of fewer bonds (Si-O-Al and Si-O-Si) that constitute geopolymers, negatively impacting compressive strength, as supported by previous studies [44]. Moreover, the lower reactivity of clay and feldspar minerals in LP, which requires a longer time for the formation of the reaction and gel structure, may contribute to the lower strength [67–70]. The nearly zero-charge layered structure of kaolinite on the surface slows down the penetration of alkalis into the structure, leading to the formation of a weak structure in most clay-based geopolymers. Kaolinite does not fully participate in the polymer structure [67,70,71]. An increase in the BFS ratio resulted in an increase in compressive strength, attributed to the high content of SiO_2 and Al_2O_3 minerals in BFS. This observation aligns with previous studies [42,72–79]. Figure 8 provides a comparison graph of the compressive strengths of the mixtures, and Figure 9 illustrates the relationship between geopolymer mixture ratios and compressive strength.

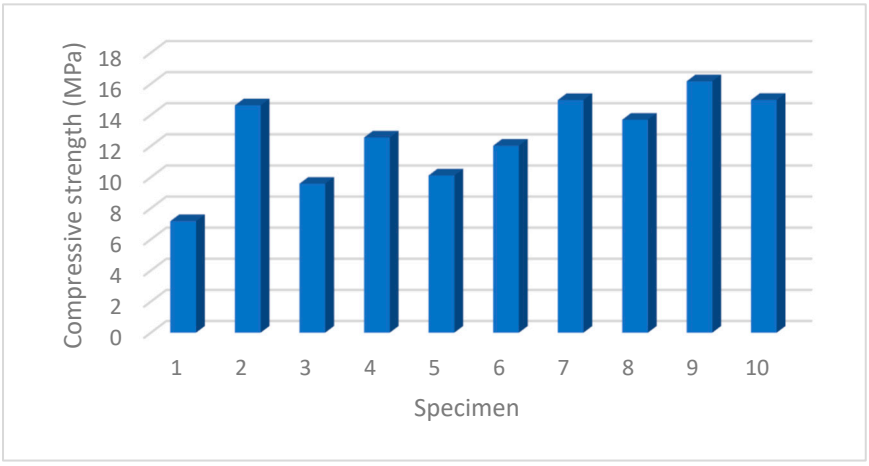

Figure 8. The compressive-strength results of the geopolymer.

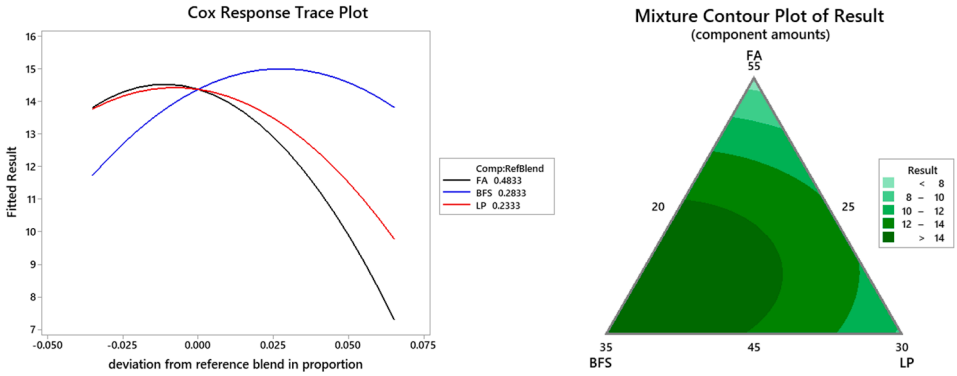

Figure 9. The correlation between the compressive-strength values and the material's mixing ratio.

3.4. Flexural Strengths

For the flexural test, three beams with dimensions of 80 × 100 × 400 mm were prepared for each mixture and flexural tests were conducted. After curing for 28 days, the beam samples were tested; the test results are presented in Table 3.

Upon examining Table 3, it is observed that the flexural strength values ranged from 1.69 to 2.9 MPa. Similar to the situation with compressive strength, an increase in the ratios of FA and LP led to a decrease in flexural strength, consistent with the findings of Taher et al. in 2021 [44]. Additionally, an increase in the BFS ratio resulted in an increase in flexural strength. The maximum flexural strength was observed in mix No. 8, with a value of 2.9 MPa, while the mixture with the lowest flexural strength was mix No. 5, with a value of 1.63 MPa. Figure 10 provides a comparison graph of the flexural strengths of the mixtures, and Figure 11 illustrates the relationship between the mixture ratios of the materials used in the geopolymer mortar and flexural strength.

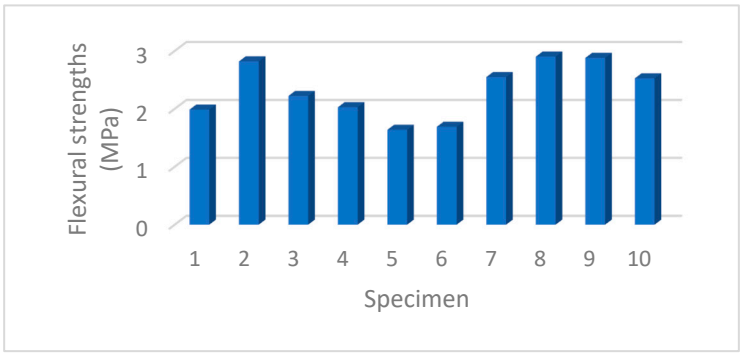

Figure 10. The flexural-strength values of the geopolymer mortar.

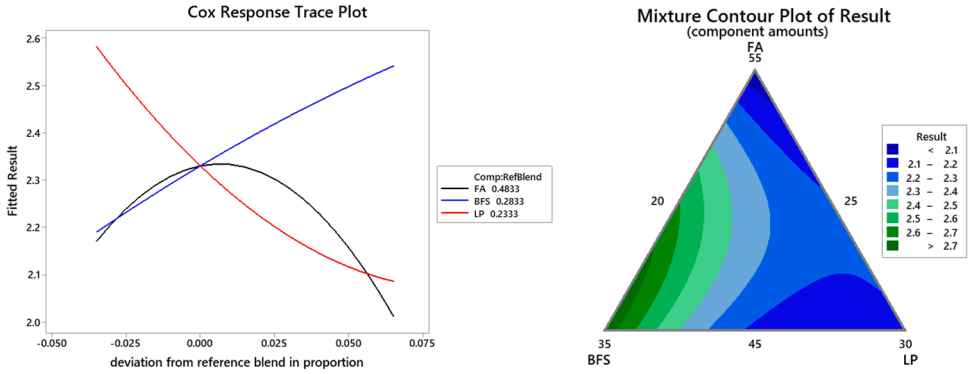

Figure 11. The relationship between the mixing ratio of the material used and the flexural-strength values.

The impact that the binding materials (FA, BFS, and LP) that were used in the production of the geopolymer mortar had on the compressive strength of the mortar was comparable to the impact they had on the flexural strength of the mortar.

3.5. Impact Resistance

To ascertain the impact resistance of concrete, the weight-dropping method, a simple and widely preferred technique, was employed. A load of 5.6 kg was released from a height of 180 mm onto a beam specimen measuring 80 × 100 × 400 mm (Figure 12). The impact energy applied to the specimens was calculated according to the formulas provided below [80,81].

The weight employed in the impact experiment was dropped from a height of 180 mm onto beam elements with dimensions of 80 × 100 × 400 mm, after a curing period of 28 days. The experimental outcomes are presented in Table 3.

$$\text{Impact resistance} = n \times U \quad (1)$$

$$H = gt^2/2 \quad (2)$$

$$U = m\,V^2/2 \quad (3)$$

$$V = g\,t \quad (4)$$

$$M = W/g \quad (5)$$

Let H stand for the height of the fall (mm), V for the hammer's impact velocity (mm/s), W for the hammer's weight (N), m for the hammer's mass (kg), g for the acceleration caused by gravity (mm/s^2), t for the hammer's fall time from a height of 180 mm, and n for the number of blows.

Figure 12. Impact test setup.

Impact experiments were conducted on specimens obtained from the prepared mixtures under identical conditions (hammer mass, weight, and height). The specimens were subjected to an impact energy of 10.02 kN/mm, calculated according to the aforementioned formulas.

Upon examining Figure 13, it is observed that the impact-resistance values of the mixtures ranged between 10 and 33.3 kNmm. Similar to compressive and flexural strength, a decrease in impact resistance was noted with the increase in the ratios of FA and LP. Simultaneously, an increase in the BFS ratio resulted in an augmentation of impact resistance. The maximum impact resistance, 33.3 kNmm, was attained in mix No. 8 and mix No. 9. The mixture yielding the lowest impact resistance was mix No. 1 with a value of 10 kNmm, as depicted in Figure 14, which illustrates the effects of the constituent materials on impact resistance.

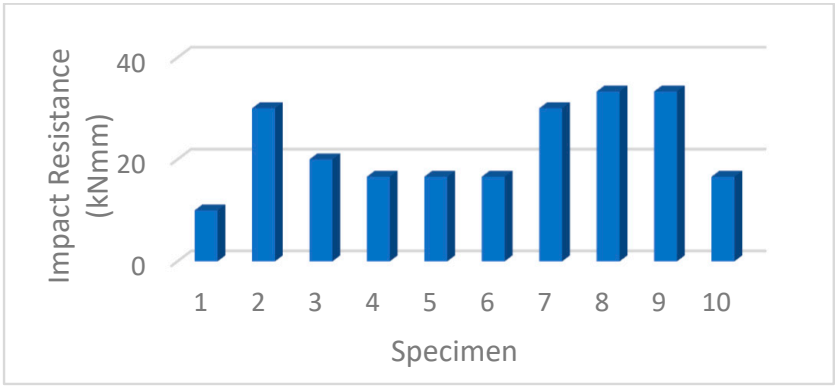

Figure 13. The impact-resistance values of the geopolymer mortar.

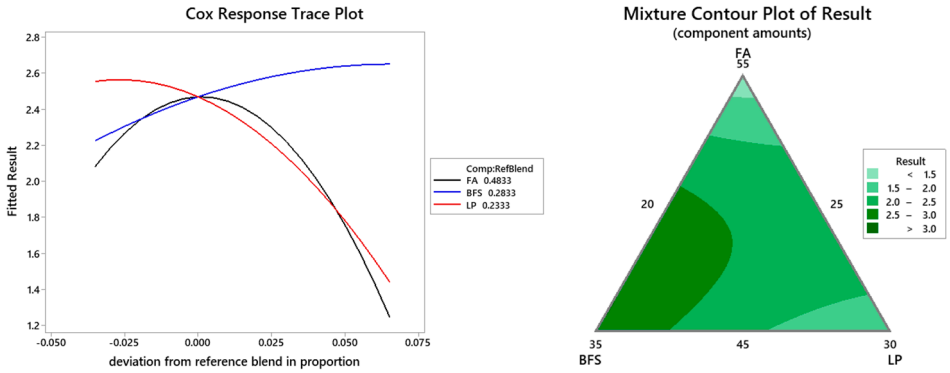

Figure 14. The connection between the mixing ratio of the material used and the impact-resistance values.

The impact resistance of the prepared geopolymer mortar aligned consistently with the factors influencing flexural and compressive strength.

3.6. Water Absorption

The water-absorption test was conducted on cylindrical specimens with dimensions of Ø100 × 50 mm, following a curing period of 28 days for geopolymers; the outcomes are shown in Table 3.

Upon examining Figure 15, it is observed that water-absorption values varied, between 8.23% and 10.17%. An increase in the FA ratio corresponded to an elevation in water-absorption values. This phenomenon was attributed to the greater surface area of fly ash compared to those of BFS and LP, necessitating a higher activator solution for exhibiting pozzolanic properties.

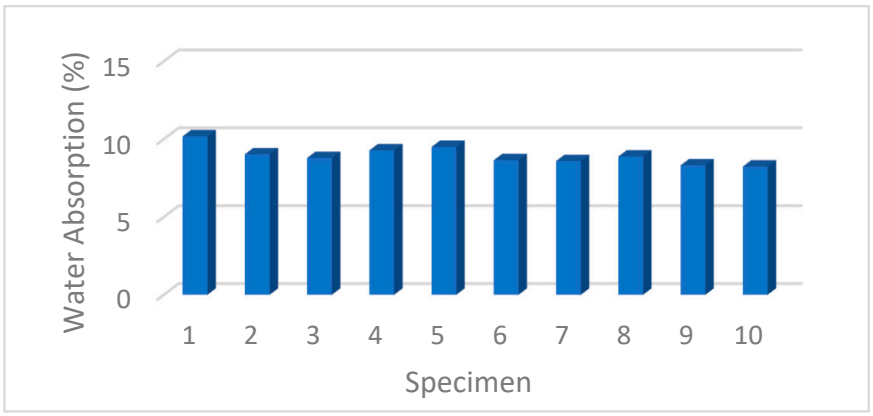

Figure 15. The water-absorption values of the geopolymer mortar.

Furthermore, the particles of BFS and LP, being smaller than those of fly ash, were noted to reduce voids in the geopolymer mix, resulting in a decrease in water absorption with increasing ratios, corroborating findings of previous studies [48]. This study supports the conclusion that the smaller size of BFS and LP particles, in comparison to fly ash, contributes to a reduction in water absorption in the geopolymer mix. The maximum water-absorption rate obtained from the experiments was 10.17% for mix No. 1, as illustrated in Figure 16, which depicts the impact of the materials constituting the mixture on water-absorption quantities.

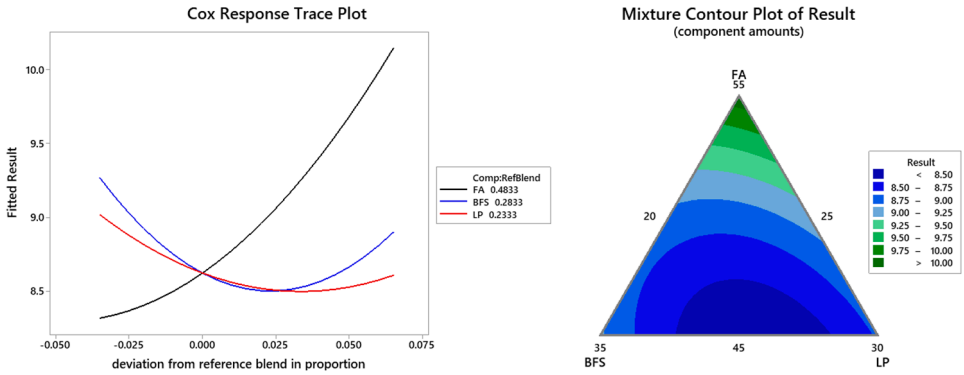

Figure 16. The relationship between the mixing ratio of the material used and the water-absorption values.

3.7. Dry Unit Weight

Within the scope of the study, geopolymer cubes of dimensions 50 × 50 × 50 mm were produced. After a curing period of 28 days, their weights were measured in a dry state (air-dried) using a precision balance, and their dry unit weights were calculated. The results are presented in Figure 17.

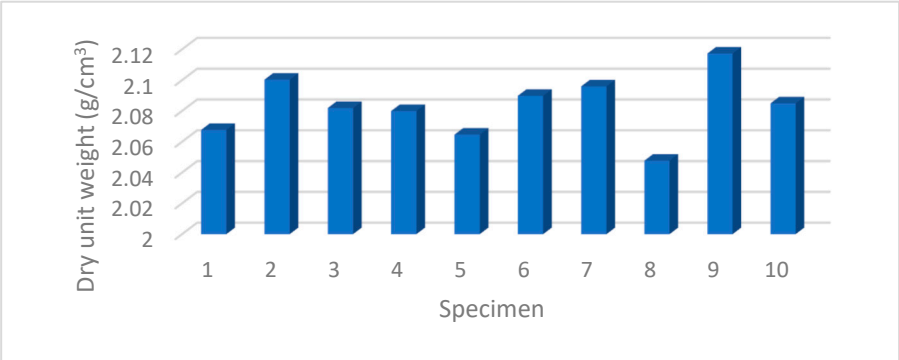

Figure 17. The dry unit weights of the geopolymer mortar.

Upon examining Figure 17, it is observed that the dry unit weight values of the mortars varied between 2.04 and 2.11 g/cm^3. The heaviest dry weight obtained from the tests was 2.11 g for every cubic centimeter in mix No. 9, as shown in Figure 18. This tells us how different materials that make up this mixture affect its density when everything is dry and not full of water (or wet).

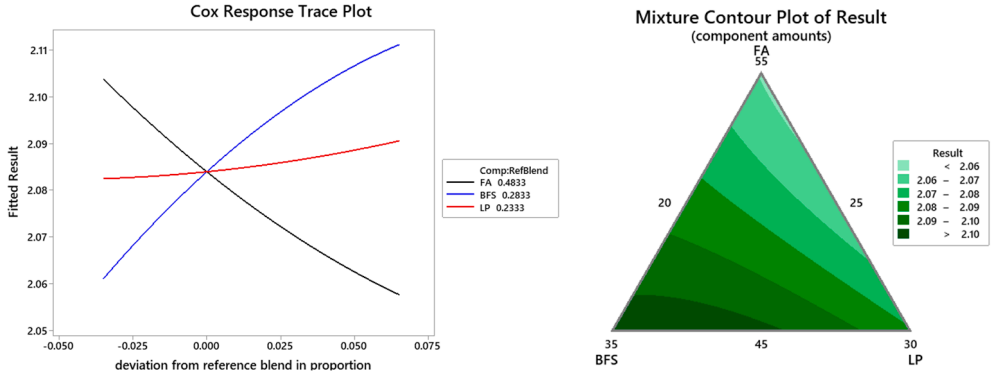

Figure 18. The relationship between the mixing ratio of the material used and the dry unit weights.

Because FA particles are bigger than the other waste materials mixed, it was noticed that the samples had more void ratios. As the amount of FA increased, a decrease in dry

unit weight was observed. This outcome matched what Kaya et al. found in 2020 [31]. The size of particles in BFS and LP is less than that in FA. This leads to making geopolymers with fewer empty spaces inside them. Therefore, it was found that as more BFS and LP were added, the dry weight increased.

The consolidated results of experiments conducted on prepared geopolymer mortars are shown in Table 3.

Upon reviewing Table 3, it is evident that sample mix No. 9, which provides the highest dry unit weight, also yields the highest compressive strength value. This is attributed to porosity; the sample with the highest porosity exhibited lower dry unit weight and compressive strength, while simultaneously presenting a higher void ratio and higher water-absorption values.

4. Conclusions

As a result of this study, which was conducted to investigate the impact of fly ash (FA), blast furnace slag (BFS), and limestone powder (LP) on the mechanical and physical characteristics of geopolymer mortar, the following conclusion were reached:

(1) An increase in FA content led to an augmentation in water absorption, accompanied by a decrease in dry unit weight, compressive strength, flexural resistance, impact resistance, and initial setting-time values.
(2) The dry unit weight, flexural strength, compressive strength, and resistance to impacts all rose significantly as the percentage of BFS in the material increased. Both the initial setup time and the amount of water that was absorbed reduced simultaneously.
(3) The properties of the material—dry unit weight, flexural strength, compressive strength, impact resistance, and water absorption—decreased as the LP content increased, while the initial setting time increased.
(4) The presence and increased quantity of LP enhanced the workability of geopolymer, due to the fineness and the spherical shape of LP particles for all prepared mixtures.
(5) The amount of additional water used in the production of geopolymer mortar was observed to be crucial and influential on its mechanical and physical properties.
(6) Despite the fixed amount of additional water in mortar production, an increase in water quantity in supplementary studies positively impacted workability but adversely affected compressive strength and the initial setting time.
(7) In the future, it is recommended that studies should concentrate on the basic science of geopolymers to discover the process of chemical reactions that occur during the procedure of setting and hardening.

5. Future Research Needs

Based on the experiences gained from this study in the production of geopolymer mortar using BFS, LP, or FA, the following recommendations will contribute to future research:

(1) As mentioned earlier, FA is classified into F and C classes, according to ASTM standards. In this study, only C-class FA was utilized. It is recommended that more studies be conducted making use of F-class FA and applying statistical approaches that are more thorough, in order to investigate the mechanical and physical characteristics of geopolymer.
(2) The FA that was used in this experiment was derived from the Soma Thermal Power Plant, which is situated in the city of Manisa in Turkey. It is recommended that similar studies be conducted using different ash samples from various thermal power plants. Because thermal power plants have varying burning potentials, the findings may be considerably impacted by these differences.
(3) In addition to the experimental studies conducted in this research, a comprehensive study could be carried out by applying other tests on geopolymer mortar, such as tests for air content, sulfate resistance, shrinkage measurement, ultrasonic transit time, elastic modulus, and abrasion resistance.

(4) The influence of mixture materials on the mechanical characteristics of geopolymer mortar could be examined for long-term curing periods.
(5) One of the major challenges in geopolymer production, identified in this study, is the short initial setting time. Since the initial setting times obtained in the study were very short, it is possible to extend the setting times by using different additive materials or chemical admixtures.
(6) Considering that Si-O-Si bonds are strong in geopolymer formation, materials with a high SiO2 ratio, such as metakaolin, silica fume, or fly ash class-F, could be used to obtain geopolymers with superior mechanical properties.

Author Contributions: Conceptualization, İ.H.E. and S.A.; methodology, İ.H.E. and S.A.; experiment, S.A.; supervision, İ.H.E.; data curation, S.A.; validation, İ.H.E.; formal analysis, S.A.; investigation, İ.H.E. and S.A.; resources, İ.H.E.; writing—original draft, S.A.; writing—review and editing, İ.H.E. All authors have read and agreed to the published version of the manuscript.

Funding: This study has received support from project number 221104056, belonging to the Scientific Research Projects (BAP) of Konya Technical University.

Institutional Review Board Statement: Not applicable.

Informed Consent Statement: Not applicable.

Data Availability Statement: The data presented in this study are available on request from the corresponding author. The data are not publicly available, due to privacy concerns.

Acknowledgments: This study was produced from Salih Aslan's Ph.D. thesis. Salih Aslan is a Ph.D. student under the guidance of İ. Hakkı Erkan as supervisor.

Conflicts of Interest: The authors declare no conflict of interest.

References

1. Davidovits, J. *False Values on CO_2 Emission for Geopolymer Cement/Concrete Published in Scientific Papers*; Technical Paper #24; Geopolymer Institute: Saint-Quentin, France, 2015; Volume 24, pp. 1–9.
2. Singh, G.B.; Subramaniam, K.V. Production and characterization of low-energy Portland composite cement from post-industrial waste. *J. Clean. Prod.* **2019**, *239*, 118024. [CrossRef]
3. Wang, J.; Dai, Y.; Gao, L. Exergy analyses and parametric optimizations for different cogeneration power plants in the cement industry. *Appl. Energy* **2009**, *86*, 941–948. [CrossRef]
4. Zhang, W.; Maleki, A.; Khajeh, M.G.; Zhang, Y.; Mortazavi, S.M.; Vasel-Be-Hagh, A. A novel framework for integrated energy optimization of a cement plant: An industrial case study. *Sustain. Energy Technol. Assess.* **2019**, *35*, 245–256. [CrossRef]
5. Demir, İ. F sınıfı uçucu kül ve yüksek fırın cürufu ikamesinin çimento harç özelliklerine etkisi. *Int. J. Eng. Res. Dev.* **2022**, *14*, 531–543.
6. Qaidi, S.M.; Atrushi, D.S.; Mohammed, A.S.; Ahmed, H.U.; Faraj, R.H.; Emad, W.; Tayeh, B.A.; Najm, H.M. Ultra-high-performance geopolymer concrete: A review. *Constr. Build. Mater.* **2022**, *346*, 128495. [CrossRef]
7. Amran, M.; Debbarma, S.; Ozbakkaloglu, T. Fly ash-based eco-friendly geopolymer concrete: A critical review of the long-term durability properties. *Constr. Build. Mater.* **2021**, *270*, 121857. [CrossRef]
8. Abdulrahman, H.; Muhamad, R.; Visintin, P.; Shukri, A.A. Mechanical properties and bond stress-slip behaviour of fly ash geopolymer concrete. *Constr. Build. Mater.* **2022**, *327*, 126909. [CrossRef]
9. Chokkalingam, P.; El-Hassan, H.; El-Dieb, A.; El-Mir, A. Development and characterization of ceramic waste powder-slag blended geopolymer concrete designed using Taguchi method. *Constr. Build. Mater.* **2022**, *349*, 128744. [CrossRef]
10. Amin, M.; Elsakhawy, Y.; Abu el-hassan, K.; Abdelsalam, B.A. Behavior evaluation of sustainable high strength geopolymer concrete based on fly ash, metakaolin, and slag. *Case Stud. Constr. Mater.* **2022**, *16*, e00976. [CrossRef]
11. Mustakim, S.M.; Das, S.K.; Mishra, J.; Aftab, A.; Alomayri, T.S.; Assaedi, H.S.; Kaze, C.R. Improvement in fresh, mechanical and microstructural properties of fly ash-blast furnace slag based geopolymer concrete by addition of nano and micro silica. *Silicon* **2021**, *13*, 2415–2428. [CrossRef]
12. Zuaiter, M.; El-Hassan, H.; El-Maaddawy, T.; El-Ariss, B. Properties of slag-fly ash blended geopolymer concrete reinforced with hybrid glass fibers. *Buildings* **2022**, *12*, 1114. [CrossRef]
13. *ASTM C618*; Standard Specification for Coal Fly Ash and Raw or Calcined Natural Pozzolan for Use as a Mineral Admixture in Concrete. Annual Book of ASTM Standards, ASTM: West Conshohocken, PA, USA, 1998.
14. Boyacı, Ö. Farklı Kaolenlerin Metakaolen ve Spinel Yapılarda Geopolimer Davranışı. Master's Thesis, Kütahya Dumlupınar University/Institute of Science, Kütahya, Turkey, 2018.

15. Bingöl, Ş. Alkali ile Aktive Edilmiş Yüksek Fırın Cürufu Geopolimer Harçların Mekanik ve Durabilite Özelliklerinin Araştırılması. Ph.D. Thesis, Erciyes University/Institute of Science, Kayseri, Turkey, 2018.
16. Zeybek, O. Uçucu kül Esaslı Geopolimer Tuğla Üretimi. Master's Thesis, Anadolu University/Institute of Science, Eskişehir, Turkey, 2009.
17. Atis, C.D.; Gorur, E.B.; Karahan, O.; Bilim, C.; Ilkentapar, S.; Luga, E. Very high strength (120 MPa) class F fly ash geopolymer mortar activated at different NaOH amount, heat curing temperature and heat curing duration. *Constr. Build. Mater.* **2015**, *96*, 673–678. [CrossRef]
18. Okoye, F.N.; Durgaprasad, J.; Singh, N.B. Fly ash/Kaolin based geopolymer green concretes and their mechanical properties. *Data Brief* **2015**, *5*, 739–744. [CrossRef] [PubMed]
19. Yu, X.; Jiang, L.; Xu, J.; Zu, Y. Effect of Na_2SiO_3 content on passivation and corrosion behavior of steel in a simulated pore solution of Na_2SiO_3-activated slag. *Constr. Build. Mater.* **2017**, *146*, 156–164. [CrossRef]
20. Chi, H.L.; Louda, P.; Bakalova, T.; Kovačič, V. Preparation and mechanical properties of potassium metakaolin based geopolymer paste. *Adv. Eng. Forum* **2019**, *31*, 38–45. [CrossRef]
21. Davidovits, J. High-Alkali cements for 21st century concretes. *Spec. Publ.* **1994**, *144*, 383–398.
22. Luhar, S.; Nicolaides, D.; Luhar, I. Fire Resistance Behaviour of Geopolymer Concrete: An overview. *Buildings* **2021**, *11*, 82. [CrossRef]
23. Komljenovic, M.; Bascarivic, Z.; Bradic, V. Mechanical and microstructural properties of alkaliactivated fly ash geopolymers. *J. Hazard. Mater.* **2010**, *181*, 35–42. [CrossRef]
24. Greiser, S.; Gluth, G.; Sturm, P.; Jäger, C. ^{29}Si {^{27}Al}, ^{27}Al {^{29}Si} and ^{27}Al{^{1}H} double-resonance NMR spectroscopy study of cementitious sodium aluminosilicate gels (geopolymers) and gel-zeolite composites. *RSC Adv.* **2018**, *70*, 40164–40171. [CrossRef]
25. Tayeh, B.A.; Hakamy, A.; Amin, M.; Zeyad, A.M.; Agwa, I.S. Effect of air agent on mechanical properties and microstructure of lightweight geopolymer concrete under high temperature. *Case Stud. Constr. Mater.* **2022**, *16*, e00951. [CrossRef]
26. Amin, M.; Zeyad, A.M.; Tayeh, B.A.; Agwa, I.S. Effect of high temperatures on mechanical, radiation attenuation and microstructure properties of heavyweight geopolymer concrete. *Struct. Eng. Mech.* **2021**, *80*, 181.
27. Ghafoor, M.T.; Khan, Q.S.; Qazi, A.U.; Sheikh, M.N.; Hadi, M.N.S. Influence of alkaline activators on the mechanical properties of fly ash based geopolymer concrete cured at ambient temperature. *Constr. Build. Mater.* **2021**, *273*, 121752. [CrossRef]
28. Tippayasam, C.; Balyore, P.; Thavorniti, P.; Kamseu, E.; Leonelli, C.; Chindaprasirt, P.; Chaysuwan, D. Potassium alkali concentration and heat treatment affected metakaolin-based geopolymer. *Constr. Build. Mater.* **2016**, *104*, 293–297. [CrossRef]
29. Ankur, G. Investigation of the strength of ground granulated blast furnace slag based geopolymer composite with silica fume. *Mater. Today Proc.* **2021**, *44*, 23–28.
30. Kaya, M.; Uysal, M.; Yılmaz, K.; Atiş, C.D. Behaviour of geopolymer mortars after exposure to elevated temperatures. *Mater. Sci.* **2018**, *24*, 428–436. [CrossRef]
31. Kaya, M.; Uysal, M.; Yilmaz, K.; Karahan, O.; Atiş, C.D. Mechanical properties of class C and F fly ash geopolymer mortars. *Gradevinar* **2020**, *72*, 297–309.
32. İlkentapar, S.; Atiş, C.D.; Karahan, O.; Görür Avşaroğlu, E.B. Influence of duration of heat curing and extra rest period after heat curing on the strength and transport characteristic ofalkali activated class F fly ash geopolymer mortar. *Constr. Build. Mater.* **2017**, *151*, 363–369. [CrossRef]
33. Ozodabas, A.; Yilmaz, K. Improvement of the performance of alkali activated blast furnace slag mortars with very finely ground pumice. *Constr. Build. Mater.* **2013**, *48*, 26. [CrossRef]
34. Atabey, İ.İ. F Sınıfı Uçucu Küllü Geopolimer Harcının Durabilite Özelliklerinin Araştırılması. Ph.D. Thesis, Erciyes University/Institute of Science, Kayseri, Turkey, 2017.
35. Balcikanli, M.; Turker, H.T.; Ozbay, E.; Karahan, O.; Atis, C.D. Identifying the bond and abrasion behavior of alkali activated concretes by central composite design method. *Constr. Build. Mater.* **2017**, *132*, 196–209. [CrossRef]
36. Kaya, M. Farklı Tür Uçucu Küller Kullanılarak Üretilen Alkali Aktive Edilmiş Harçların Mekanik ve Durabilite Özelliklerinin Incelenmesi. Ph.D. Thesis, Sakarya Universitesi, Sakarya, Turkey, 2016.
37. Zhang, M.; Zhao, M.; Zhang, G.; Mann, D.; Lumsden, K.; Tao, M. Durability of red mud-fly ash based geopolymer and leaching behavior of heavy metals in sulfuric acid solutions and deionized water. *Constr. Build. Mater.* **2016**, *124*, 373–382. [CrossRef]
38. Jindal, B.B. Investigations on the properties of geopolymer mortar and concrete with mineral admixtures: A review. *Constr. Build. Mater.* **2019**, *227*, 116644. [CrossRef]
39. Aktürk, M. Metakaolin Tabanlı Pişirilmiş Taş Tozu Atığı Ikameli Kolemanit Ve Boraks Penta Hidrat Katkılı Geopolimer Harçların Fiziksel Ve Mekanik Özellikleri. Ph.D. Thesis, Faculty of Engineering and Natural Sciences, Konya Technical University, Konya, Turkey, 2021.
40. Kotwal, A.R.; Kim, Y.J.; Hu, J.; Sriraman, V. Characterization and early age physical properties of ambient cured geopolymer mortar based on class C fly ash. *Int. J. Concr. Struct. Mater.* **2015**, *9*, 35–43. [CrossRef]
41. Sasui, S.; Kim, G.; Nam, J.; Koyama, T.; Chansomsak, S. Strength and microstructure of class-C fly ash and GGBS blend geopolymer activated in NaOH & NaOH+ Na_2SiO_3. *Materials* **2019**, *13*, 59.
42. Kumar, S.; Kumar, R.; Mehrotra, S.P. Influence of granulated blast furnace slag on the reaction, structure and properties of fly ash based geopolymer. *J. Mater. Sci.* **2010**, *45*, 607–615. [CrossRef]

43. Kürklü, G. The effect of high temperature on the design of blast furnace slag and coarse fly ash-based geopolymer mortar. *Compos. Part B Eng.* **2016**, *92*, 9–18. [CrossRef]
44. Taher, S.M.; Saadullah, S.T.; Haido, J.H.; Tayeh, B.A. Behavior of geopolymer concrete deep beams containing waste aggregate of glass and limestone as a partial replacement of natural sand. *Case Stud. Constr. Mater.* **2021**, *15*, e00744. [CrossRef]
45. Kubátová, D.; Khongová, I.; Kotlanova, M.K.; Zezulova, A.; Bohac, M. The use of limestone sludge for the geopolymer preparation. In *IOP Conference Series: Materials Science and Engineering, Proceedings of the International Conference Building Materials, Products and Technologies (ICBMPT 2021), Telc, Czech Republic, 29September–1st October 2021*; IOP Publishing: Bristol, UK, 2021; Volume 1205, p. 012002.
46. Bayiha, B.N.; Billong, N.; Yamb, E.; Kaze, R.C.; Nzengwa, R. Effect of limestone dosages on some properties of geopolymer from thermally activated halloysite. *Constr. Build. Mater.* **2019**, *217*, 28–35. [CrossRef]
47. Minitab Inc. Minitab Software for Quality Improvement. Available online: www.minitab.com (accessed on 18 May 2023).
48. Shi, C.; Roy, D.; Krivenko, P. *Alkali-Activated Cements and Concretes*; CRC Press: Boca Raton, FL, USA, 2003.
49. Taji, I.; Ghorbani, S.; de Brito, J.; Tam, V.W.; Sharifi, S.; Davoodi, A.; Tavakkolizadeh, M. Application of statistical analysis to evaluate the corrosion resistance of steel rebars embedded in concrete with marble and granite waste dust. *J. Clean. Prod.* **2019**, *210*, 837–846. [CrossRef]
50. Tahwia, A.M.; Hamido, M.A.; Elemam, W.E. Using mixture design method for developing and optimizing eco-friendly ultra-high performance concrete characteristics. *Case Stud. Constr. Mater.* **2023**, *18*, e01807. [CrossRef]
51. Altawil, H.A.H. Geopolimer Kazıkların Üretimi ve Performansını Etkileyen Faktörlerin Deneysel Olarak Araştırılması. Ph.D. Thesis, Faculty of Engineering and Natural Sciences, Konya Technical University, Konya, Turkey, 2022.
52. *ASTM C 403/C 403M*; Test Method for Time of Setting of Concrete Mixtures by Penetration Resistance (C 403/C 403M). Annual Book of ASTM Standards, ASTM International: West Conshohocken, PA, USA, 2003.
53. *ASTM, C230/C230M-14*; Standard Specification for Flow Table for Use in Tests of Hydraulic Cement. ASTM International: West Conshohocken, PA, USA, 2014.
54. *ASTM C39–05*; Standard Test Method for Compressive Strength of Cylindrical Concrete Specimens. Annual book of ASTM Standards: West Conshohocken, PA, USA, 2005.
55. *ASTM C293*; Standard Test Method for Flexural Strength of Concrete (Using Simple Beam with Center Point Loading). Annual Book of ASTM Standard: West Conshohocken, PA, USA, 1979.
56. ACI Committee 544. *Report on Fiber Reinforced Concrete (ACI 544.1R-96) (Reapproved 2009)*; American Concrete Institute: Farmington Hills, MI, USA, 1996; p. 66.
57. *ASTM C642–13*; Standard Test Method for Density, Absorption, and Voids in Hardened Concretes. ASTM International: West Conshohocken, PA, USA, 2013.
58. Yildiz, S. Endüstriyel Yan Ürünlerle Üretilmiş Geopolimer Betonların Mekanik Ve Durabilite Özelliklerinin Araştırılması. Ph.D. Thesis, Kocaeli University, İzmit, Turkey, 2023.
59. Qiu, J.; Zhao, Y.; Xing, J.; Sun, X. Fly ash/blast furnace slag-based geopolymer as a potential binder for mine backfilling: Effect of binder type and activator concentration. *Adv. Mater. Sci. Eng.* **2019**, *2019*, 2028109. [CrossRef]
60. Bernal, S.A.; San Nicolas, R.; Van Deventer, J.S.; Provis, J.L. Alkali-activated slag cements produced with a blended sodium carbonate/sodium silicate activator. *Adv. Cem. Res.* **2016**, *28*, 262–273. [CrossRef]
61. Nath, P.; Sarker, P.K. Effect of GGBFS on setting, workability and early strength properties of fly ash geopolymer concrete cured in ambient condition. *Constr. Build. Mater.* **2014**, *66*, 163–171. [CrossRef]
62. Li, Z.; Li, S. Carbonation Resistance of Fly Ash and Blast Furnace Slag Based Geopolymer Concrete. *Constr. Build. Mater.* **2018**, *163*, 668–680. [CrossRef]
63. Nuaklong, P.; Sata, V.; Chindaprasirt, P. Influence of Recycled Aggregate on Fly Ash Geopolymer Concrete Properties. *J. Clean. Prod.* **2016**, *112*, 2300–2307. [CrossRef]
64. Malkawi, A.B.; Nuruddin, M.F.; Fauzi, A.; Almattarneh, H.; Mohammed, B.S. Effects of Alkaline Solution on Properties of The HCFA Geopolymer Mortars. *Procedia Eng.* **2016**, *148*, 710–717. [CrossRef]
65. Nath, P.; Sarker, P.K. Use of OPC to Improve Setting and Early Strength Properties of Low Calcium Fly Ash Geopolymer Concrete Cured at Room Temperature. *Cem. Concr. Compos.* **2015**, *55*, 205–214. [CrossRef]
66. Yuan, B.; Yu, Q.L.; Brouwers, H.J.H. Assessing the chemical involvement of limestone powder in sodium carbonate activated slag. *Mater. Struct.* **2017**, *50*, 136. [CrossRef]
67. Xu, H.; Van Deventer, J.S.J. The geopolymerisation of alumino-silicate minerals. *Int. J. Miner. Process.* **2000**, *59*, 247–266. [CrossRef]
68. Komnitsas, K.; Zaharaki, D.; Perdikatsis, V. Geopolymerisation of low calcium ferronickel slags. *J. Mater. Sci.* **2007**, *42*, 3073–3082. [CrossRef]
69. Van Jaarsveld, J.G.S.; van Deventer, J.S.J.; Lukey, G.C. The effect of composition and temperature on the properties of fly ash-and kaolinite-based geopolymers. *Chem. Eng. J.* **2002**, *89*, 63–73. [CrossRef]
70. Liew, Y.M.; Heah, C.Y.; Mohd Mustafa, A.B.; Kamarudin, H. Structure and properties of clay-based geopolymer cements: A review. *Prog. Mater. Sci.* **2016**, *83*, 595–629. [CrossRef]
71. Heah, C.Y.; Kamarudin, H.; Mustafa Al Bakri, A.M.; Bnhussain, M.; Khairul Nizar, I.; Ruzaidi, C.M.; Liew, Y.M. Study on solids-to-liquid and alkaline activator ratios on kaolin-based geopolymers. *Constr. Build. Mater.* **2012**, *35*, 912–922. [CrossRef]

72. Ravikumar, D.; Neithalath, N. Effects of activator characteristics on the reaction product formation in slag binders activated using alkali silicate powder and NaOH. *Constr. Build. Mater.* **2012**, *34*, 809–818. [CrossRef]
73. Fernández-Jiménez, A.; Puertas, F.; Sobrados, I.; Sanz, J. Structure of calcium silicate hydrates formed in alkaline-activated slag: Influence of the type of alkaline activator. *J. Am. Ceram. Soc.* **2003**, *86*, 1389–1394. [CrossRef]
74. Wang, W.C.; Wang, H.Y.; Lo, M.H. The fresh and engineering properties of alkali activated slag as a function of fly ash replacement and alkali concentration. *Constr. Build. Mater.* **2015**, *84*, 224–229. [CrossRef]
75. Puertas, F.; Martínez-Ramírez, S.; Alonso, S.; Vazquez, T. Alkali-activated fly ash/slag cements: Strength behaviour and hydration products. *Cem. Concr. Res.* **2000**, *30*, 1625–1632. [CrossRef]
76. Buchwald, A.; Hilbig, H.; Kaps, C. Alkali-activated metakaolin-slag blends—Performance and structure in dependence of their composition. *J. Mater. Sci.* **2007**, *42*, 3024–3032. [CrossRef]
77. Buchwald, A.; Tatarin, R.; Stephan, D. Reaction progress of alkaline-activated metakaolin-ground granulated blast furnace slag blends. *J. Mater. Sci.* **2009**, *44*, 5609–5617. [CrossRef]
78. Yao, X.; Zhang, Z.; Zhu, H.; Chen, Y. Geopolymerization process of alkali–metakaolinite characterized by isothermal calorimetry. *Thermochim. Acta* **2009**, *493*, 49–54. [CrossRef]
79. Mozgawa, W.; Deja, J. Spectroscopic studies of alkaline activated slag geopolymers. *J. Mol. Struct.* **2009**, *924*, 434–441. [CrossRef]
80. Murali, G.; Santhi, A.S.; Ganesh, G.M. Effect of crimped and hooked end steel fibres on the impact resistance of concrete. *J. Appl. Sci. Eng.* **2014**, *17*, 259–266.
81. Oltulu, M.; Gökhan Altun, M. Betonun darbe dayanımının tespitinde ağırlık düşürme deney yöntemi ve yapılan çalışmalar. *Gümüşhane Univ./Fen Bilim. Derg.* **2018**, *8*, 155–163.